PROPERTIES OF MAGNETIC FEATURES FROM THE ANALYSIS OF NEAR-INFRARED SPECTRAL LINES

SAMI K. SOLANKI
Institute of Astronomy, ETH-Zentrum, CH-8092 Zürich, Switzerland

Abstract. An overview is given of the structure and the physics of magnetic features in solar plages, as derived from observations of near-infrared lines. First, the diagnostic potential of near-infrared lines is compared with that of lines in the visible and at 12 μm. Then, the results on the magnetic and velocity structure of magnetic features obtained from 1.5 μm lines are described, discussed and compared with results of observations in the visible and with theoretical predictions. Finally, the past and present achievements of near-infrared investigations of Zeeman-split lines are summarized.

Key words: infrared: stars – Sun: faculae, plages – Sun: magnetic fields

1. Introduction

Of the many branches of solar research that have been enriched by investigations of infrared radiation, none has been transformed to the same extent as the measurement of magnetic fields. The opening of the infrared has qualitatively enhanced our capability of studying magnetic features. It is, therefore, a pleasant task to review results obtained in solar plages using near-infrared lines, which, in the context of the present review, implies lines with wavelengths between 1.5 and 1.8 μm (magnetic fields in solar plages have very rarely been observed in other near-infrared wavelength ranges, but see, *e.g.*, Harvey and Hall 1971). I shall concentrate on describing and discussing the information which has been derived from the observations using simple models. Thus, the present review concentrates on the interface between observation and theory, each of which is reviewed very competently elsewhere in the present volume (Rabin 1993 and Steiner 1993, respectively).

2. Comparison Between Visible, 1.5 μm and 12 μm Spectral Lines

The most obvious difference between the three wavelength ranges, as far as diagnostics based on the Zeeman-effect are concerned, is in the sensitivity of the spectral lines to the magnetic field (Zeeman sensitivity). The ratio of Zeeman splitting, $\Delta\lambda_H$, to non-magnetic line width, $\Delta\lambda_D$, determines the Zeeman sensitivity: $\Delta\lambda_H/\Delta\lambda_D$. Since $\Delta\lambda_D$ is roughly proportional to the central wavelength of the line, λ, while $\Delta\lambda_H \sim g\lambda^2$, where g is the Landé factor, we have approximately $\Delta\lambda_H/\Delta\lambda_D \sim g\lambda$. The largest g value, $g_{\max}$ and $g_{\max}\lambda$ are listed in Table 1 for each of the three wavelength regions. The Zeeman sensitivity translates directly into the smallest field strength, $B_{\min}$, measurable using different techniques (Table 1). The line-ratio technique mentioned in the table is based on the ratio between the V profiles of two lines that are almost identical except for their g values (Stenflo 1973). Solanki *et al.* (1992*a*) showed that by a judicious choice of lines at 1.5 μm, the smallest field strength measurable with the line-ratio technique can be lowered to a value otherwise only achievable with the 12 μm lines. Unfortunately, all the strong emission lines at 12 μm have $g = 1$, so that their ratios have no value as

D. M. Rabin et al. (eds.), Infrared Solar Physics, 393–405.

TABLE I
Diagnostic properties of Zeeman-sensitive lines

Property	Visible	1.5 μm	12 μm
g_{max}	3	3	1
$g_{max} \cdot \lambda$	≈ 1.6	≈ 4.7	≈ 12.3
B_{min} from:			
a) complete splitting	1500–2000 G	400–600 G	150–200 G
b) profile fits	800–1000 G	250–300 G	$\lesssim 100$ G
c) line ratios	300–500 G	≈ 100 G	—
τ_{5000} of formation	10^{-2}	$\gtrsim 10^{-1}$	10^{-3}–10^{-4}
$\Delta B/B$ in umbra	3–5%	2–4%	—
$\Delta B/B$ in penumbra	5–25%	2–5%	0.5–2%
$\Delta B/B$ in kG flux tubes	10–15%	1–4%	5–10%
line formation	mainly LTE	LTE	NLTE

field-strength diagnostics. The three wavelength ranges also differ in the formation heights of their Zeeman-sensitive lines. Representative values are given in Table 1.

Rough estimates of the best achievable accuracy, $\Delta B/B$, in each wavelength range are given in Table 1 as well. For small-scale kG fields the *relative* accuracy at 1.5 μm is better than at 12 μm, since the field at the low height of formation of the 1.5 μm line is 4–8 times stronger than at the formation height of the 12 μm lines. Table 1 also lists whether the lines are formed in LTE or NLTE (more on the formation of the 12 μm lines can be found in the reviews by Avrett 1993 and Rutten and Carlsson 1993). Lines formed in LTE are generally simpler to interpret. Finally, let me mention two points not listed in Table 1.

1. The temperature sensitivity of the continuum intensity decreases rapidly with increasing wavelength, so that the problems posed by stray light in sunspots and by the unknown continuum intensity of magnetic elements are greatly reduced in the infrared.
2. The visible is rich in spectral lines with different temperature and velocity sensitivities. Thus these quantities can be reliably diagnosed in conjunction with the magnetic field. At 1.5 μm most of the atomic lines are temperature insensitive. Although this improves the accuracy of the measured magnetic vector, it is a substantial disadvantage for the study of the thermodynamics within magnetic features. At 12 μm the choice of lines is even smaller. Although the Mg I emission lines are known to be temperature sensitive, their temperature behavior has not yet been studied in sufficient detail.

3. Field Strengths from 1.5 μm Spectra

In a truly pioneering piece of work, Harvey and Hall (1975) made the first solar field-strength measurement using an infrared line (*cf.* Harvey 1977). They used Stokes V profiles (*i.e.*, spectra in net circular polarization) of the $g = 3$, Fe I 1.5648

μm line (in the following, referred to simply as "the $g = 3$ line"). The large Zeeman sensitivity of this line allowed the first measurement of B outside sunspots directly from the Zeeman splitting. Harvey and Hall obtained field strengths between 1.2 and 1.7 kG and thus confirmed the dominance of kG fields, suggested by earlier painstaking analysis of visible spectra (*e.g.*, Howard and Stenflo 1972, Stenflo 1973, *cf.* Beckers and Schröter 1968, Harvey *et al.* 1972).

For over a decade no further investigations using the near infrared for solar magnetic measurements were reported, although stellar investigators were not idle in the interval (see Saar 1993). Then, in 1986 Sun *et al.*, using only spectra in unpolarized light (Stokes I), confirmed the kG fields in sunspots and plages. They did find one plage region with 600 G, but it is unclear whether this low value is real or is due to uncertainties introduced into the technique due to the unavailability of Stokes Q, U and V. Sun *et al.* (1986) were mainly interested in testing the viability of 1.5 μm lines for stellar magnetic measurements, for which only Stokes I can be used (Saar 1993).

Stenflo *et al.* (1987*b*) analyzed the center-to-limb variation (CLV) of Stokes V of the $g = 3$ line. They found that the Zeeman splitting decreases measurably towards the limb, from which they concluded that B decreases with height, z, but did not determine $B(z)$ quantitatively. Note that lines in the visible are too Zeeman insensitive to allow magnetic gradients to be obtained from their CLV (Solanki *et al.* 1987).

Zayer *et al.* (1989) fitted observed Stokes V profiles of the $g = 3$ line and of Fe I 1.5822 μm (effective Landé factor $g_{\rm eff} = 0.75$) using synthetic profiles formed in flux-tube models. By simultaneously fitting these two lines, which differ mainly in their Landé factors, they were able to separate the influence of the thermodynamics from that of the magnetic field and thereby could diagnose the range of field-strengths in the spatial resolution element. Furthermore, by combining these lines with Zeeman-sensitive lines in the visible, which are formed higher in the atmosphere, they could also distinguish between horizontal and vertical magnetic gradients and thus deduce the magnetic stratification in small magnetic elements. Their results confirmed the basic theoretical picture (*e.g.*, Knölker *et al.* 1988, Steiner and Pizzo 1989) that small-scale fields are concentrated in flux tubes, whose kG fields are confined by gas pressure. They also found evidence for a weak field (400–800 G), carrying 3–7% of the flux, but, unfortunately, their analysis was restricted to only two infrared spectra.

Muglach and Solanki (1992) carried out a statistical analysis involving all unblended Fe I lines in the wavelength range 1.5–1.8 μm and confirmed the results of Zayer *et al.* (1989). They also found that for the kG fields of magnetic elements, lines with $g_{\rm eff} \gtrsim 1.5$ are completely split. To illustrate this, the wavelength separations between the red and blue Stokes V peaks, $\lambda_r - \lambda_b$, of all the analyzed lines are plotted in Figure 1 *vs.* the normalized Zeeman splitting v_H/B (*i.e.*, basically *vs.* $g_{\rm eff}$). The diamond in the upper right-hand corner is the $g = 3$ line. Only a single infrared spectrum was analyzed.

The investigations by Livingston (1991), Rabin *et al.* (1991) and Rabin (1992*a,b*) heralded a new era of plage magnetic field measurements. Mainly due to improved detectors, profiles could now be easily and reliably measured at many positions

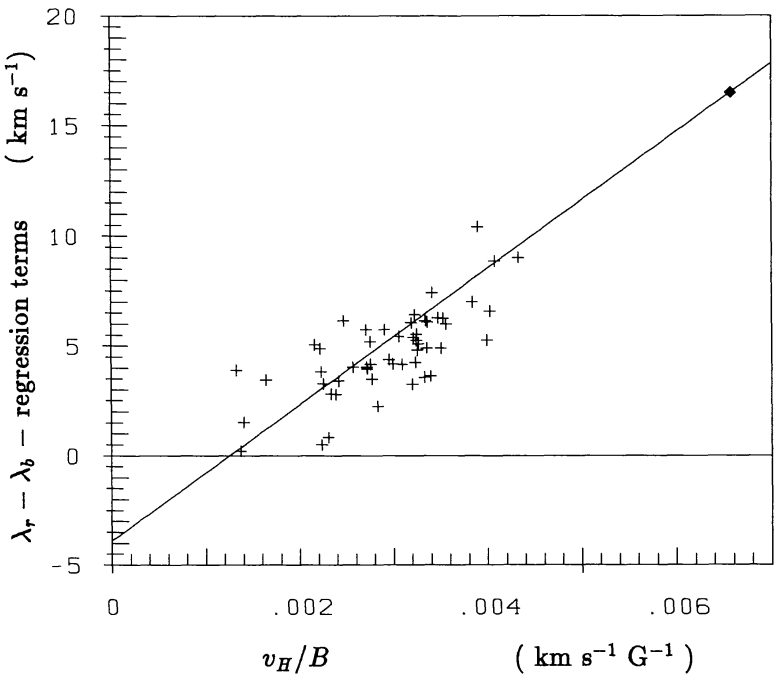

Fig. 1. Difference between the wavelengths of the red and blue Stokes V maxima, $\lambda_r - \lambda_b$ (in km s^{-1}), of all unblended Fe I lines in the 1.5–1.8 μm band *vs.* v_H/B. The non-magnetic influences on $\lambda_r - \lambda_b$ have been removed with a multivariate regression. The slope of the diagonal line corresponds to the splitting induced by 1,550 G. The diamond in the upper-right corner represents the $g = 3$ line at 1.5648 μm.

on the Sun and the variation of B from one position to the next analyzed. Most profiles gave kG fields, but smaller field strengths were also observed. In addition, many (in the case of Livingston's data), or at least some (for Rabin's data), of the observed V profiles of the $g = 3$ line had highly anomalous shapes. The solid curve in Figure 3 (left frame) shows an example of an anomalous V profile from the data set of Livingston (1991), while a normal V profile is plotted for comparison in Figure 2. Before further progress could be made, the nature of these anomalously shaped profiles had to be explained.

To find such an explanation was one of the aims of Rüedi *et al.* (1992*a*). Like Zayer *et al.* (1989) they used numerical solutions of the Unno-Rachkovsky equations obtained in flux-tube models to fit 27 V spectra of λ 1.5648 μm ($g = 3$) and λ 1.5652 μm ($g_{\rm eff} = 1.53$). They found that all V profiles (both the normally and the anomalously shaped ones) are well reproduced by standard flux-tube models. A single magnetic flux-tube component is generally sufficient to fit the normal profiles, while the anomalously shaped profiles require two separate flux-tube components. Examples of the fits to normal and anomalous profiles are shown in Figures 2 and 3, respectively. Note that in Figure 2 the adopted flux-tube model, with $B(z = 0) = 1,520$ G, not only reproduces the larger splitting of the $g = 3$ line, but also its larger σ-component width without requiring any *ad hoc* broadening. The σ-

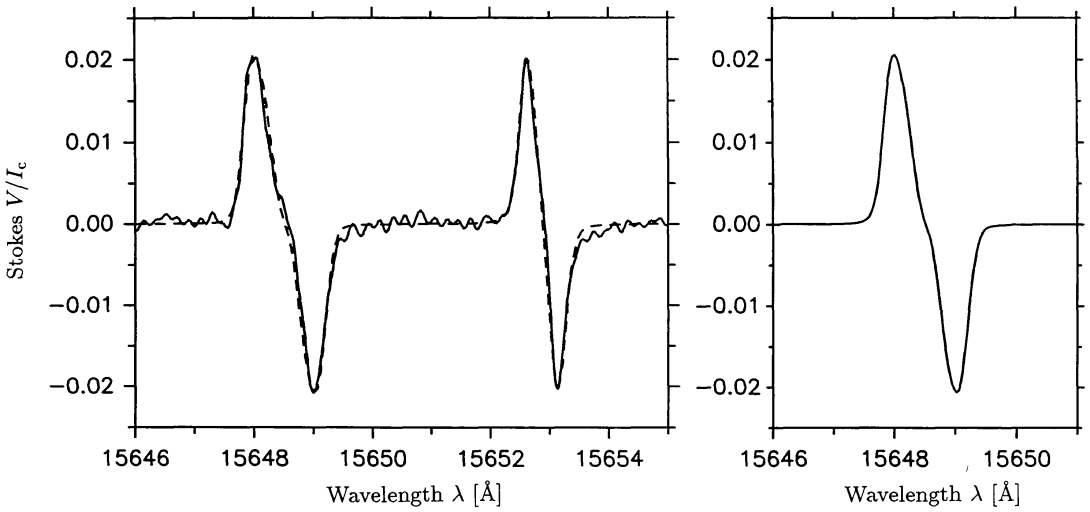

Fig. 2. a) Observed (solid) and synthetic (dashed) "normal" Stokes V profiles of Fe I 1.5648 μm ($g = 3$) and Fe I 1.5652 μm ($g_{\rm eff} = 1.53$). The synthetic profile results from a model composed of a single thin magnetic flux tube with field strength $B(z = 0) = 1,520$ G. $z = 0$ refers to unit optical depth at 0.5 μm in the quiet Sun. b) Synthetic profile of the $g = 3$ line.

component is broadened by the vertical field-strength gradient naturally introduced into the model by horizontal pressure balance. The observed profiles in Figure 3 are best fit by two flux-tube components having $B(z = 0) = 1,700$ G and $-1,080$ G, respectively, and possessing no relative Doppler shift.

Rüedi *et al.* (1992*a*) also found that approximately 90% of the magnetic flux visible in Stokes V of the $g = 3$ line is in strong-field form, *i.e.*, with $B(z = 0) \gtrsim 1,250$ G, or, equivalently, $\beta(z = 0) \leq 1$ (plasma $\beta = 8\pi P/B^2$, where P is the gas pressure). This result agrees well with the lower limit of 90% on strong-field flux set by Howard and Stenflo (1972) and Frazier and Stenflo (1972). A new feature is the definite detection of weak fields: 10% of the magnetic flux is found to have 400 G $\lesssim B(z = 0) \lesssim 1,250$s G, *i.e.*, $\beta(z = 0) > 1$. Note that $B(z = 0) \approx 400$ G corresponds to the smallest B reliably measurable with the observed line pair. Thus available observations cannot rule out the existence of still weaker fields. Figure 4 shows $B(z = 0)$ *vs.* the spatially averaged field strength. The results of fits to simple profiles are represented by circles, complex profiles by plusses (each magnetic component is represented by a separate '+'). The solid line is a regression through the strong fields.

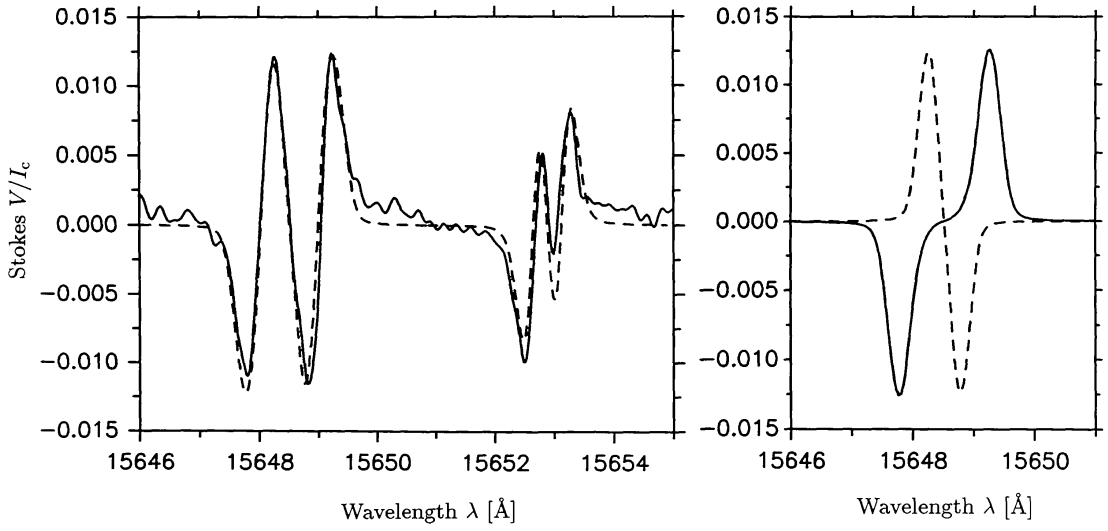

Fig. 3. a) Same as Figure 2, but for "anomalous" Stokes V profiles with strong inversions in their cores. The synthetic (dashed) curve results from two flux-tube components having opposite polarities [$B_1(z = 0) = 1,700$ G, $B_2(z = 0) = -1,050$ G] and no relative wavelength shift. b) Synthetic Stokes V profiles of each individual flux-tube component. Solid curve: V profile due to the B_1 component; dashed curve: V profile resulting from the B_2 component.

Figure 4 is in good agreement with the results of Rabin (1992*a,b*): strong fields are found at all fluxes, but intrinsically weak fields are limited to small fluxes. Thus all measurements suggest a large empty region in the lower right part of the B *vs.* $\langle B \rangle$ diagram.

How do the near-infrared results compare with theory and with observations in the visible? The solid vertical bar to the right of Figure 4 indicates the range of $B(z = 0)$ found by Zayer *et al.* (1990), based on the line ratio between λ5250.2 Å and λ5247.1 Å. The agreement between the infrared and visible results is surprisingly good for the strong fields. However, the Zeeman sensitivity of the visible lines is insufficient to measure the strength of the intrinsically weak fields. The dashed vertical bar in Figure 4 represents the theoretical predictions of Spruit (1979). He calculated the convective collapse of an initially weak field into a final, convectively stable strong field. The good agreement of the theoretical predictions with the measured strong fields suggests that kG flux tubes are indeed formed by the convective collapse of weaker fields. Convective instability and collapse have been investigated or reviewed by, *e.g.*, Parker (1978), Webb and Roberts (1978), Hasan (1984, 1985), Schüssler (1990) and Thomas (1990).

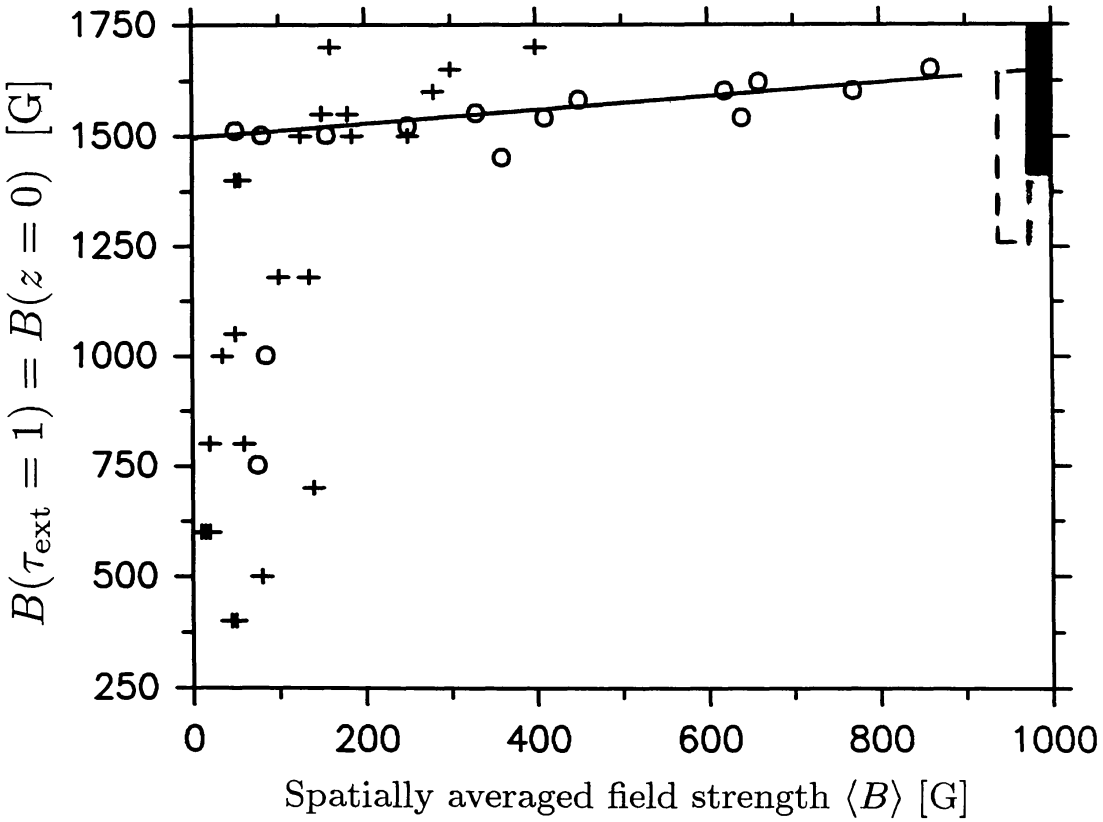

Fig. 4. $B(z = 0)$ *vs.* $\langle B \rangle$, the field strength averaged over the spatial resolution element, for all the regions analyzed by Rüedi *et al.* (1992*a*). If two magnetic components are needed to fit the observed profile, then $B(z = 0)$ for each component is plotted (denoted by a '+'). $B(z = 0)$ values obtained from single magnetic components are marked by a 'o'.

One of the major questions raised by the 1.5 μm observations concerns the nature of the weak fields. Three possible answers come to mind.

1. The weak fields may be attached to the strong fields in the form of return flux, *i.e.*, field lines that bend over and return to the solar interior close to the parent flux tube. Return-flux models of flux tubes were proposed by Frazier and Stenflo (1972) and first constructed by Osherovich (1982). Observational support for some form of return flux associated with plage flux tubes has been claimed by Koutchmy (1991) and Koutchmy *et al.* (1991). However, this interpretation of the weak fields can be ruled out by the following arguments: a) The observed weak-field component has the same polarity as the closest strong field just as often as it has the opposite polarity. This is in contrast to the return-flux model, which predicts that the weak-field component must always have the opposite polarity to the strong field. b) A weak-field component is sometimes seen without any nearby strong field.

2. At least some of the weak fields seen in the infrared data may be connected to sunspots. Solanki *et al.* (1992*b*) have shown that, near sunspots, the *super*penumbral canopy (*i.e.*, the almost horizontal magnetic field lines forming the sunspot super-

penumbra and overlying field-free gas, Giovanelli 1980) can produce a signal similar to the weak fields studied by Rüedi *et al.* (1992*a*).

3. A straightforward interpretation is that the weak fields form discrete magnetic features. Although the present observations cannot definitely confirm the existence of such "weak-field flux tubes", they do allow us to constrain their possible properties. From the field strength and the smallest measured flux an upper limit of 350–500 km can be set on the diameters of the smallest such features. Since for the weak-field features $\beta > 1$, their internal energetics are dominated by the gas (in contrast to the strong-field features, for which on average $\langle\beta\rangle \approx 0.32$, so that the magnetic energy density dominates over the internal energy density of the gas). In addition, for most weak fields $\beta > 1.8$, so that according to Spruit and Zweibel (1979) they are convectively unstable and ought to be undergoing a convective collapse, which should be visible as a redshift of the weak-field V profiles. However, no such redshifts are seen in at least nine out of twelve cases analyzed by Rüedi *et al.* (1992*a*). This implies that the weak fields must be relatively long lived and relatively stable against the convective instability. U-shaped loops (Spruit *et al.* 1987) are expected to satisfy these observational constraints and may well be responsible for the observed weak fields.

4. Velocity from 1.5 μm Spectra

4.1. The 1.5 μm Downflow Problem and its Resolution

Newer Stokes V observations in the visible show no downflows $\gtrsim 0.20$ km s^{-1} in small-scale magnetic features (*e.g.*, Stenflo and Harvey 1985, Solanki 1986, Stenflo *et al.* 1987*a*, Wiehr 1987, Solanki and Pahlke 1988, Fleck 1991). The sizable downflows suggested by older observations (*e.g.*, Giovanelli and Slaughter 1978, Wiehr 1985) turned out to be an artifact, produced by the blue-red asymmetry of the V profiles, of the low spectral resolution of these observations (Solanki and Stenflo 1986).

In the near infrared the situation has been clarified only very recently. The earliest measurements of the $g = 3$ line at 1.56 μm suggested an average downflow of 1.6 km s^{-1} in magnetic elements (Harvey 1977), although Harvey later repeatedly pointed out that deficiencies in the instrumentation may well have been responsible for the large observed wavelength shifts. A remeasurement of this line using improved instrumentation (the FTS polarimeter) resulted in a lower downflow velocity of 0.6 km s^{-1} (Stenflo *et al.* 1987*b*), which, however, still lies well outside the limit set in the visible. Recently Muglach and Solanki (1992) reanalyzed the data set of Stenflo *et al.* (1987*b*), but instead of considering only the $g = 3$ line, they investigated all the unblended Fe lines in the 1.5–1.8 μm spectral range of the data. They found no sign of a stationary flow in the observed magnetic features (Fig. 5). They also found that the uncertainty in the zero-crossing wavelength of the $g = 3$ line is of the same order as its measured shift (0.5 km s^{-1}). The large uncertainty is an indirect result of its large Zeeman splitting.

A combination of 1.5 μm and visible observations suggests that in general no stationary flows $\gtrsim 200$ m s^{-1} are present in all the photospheric layers of magnetic elements.

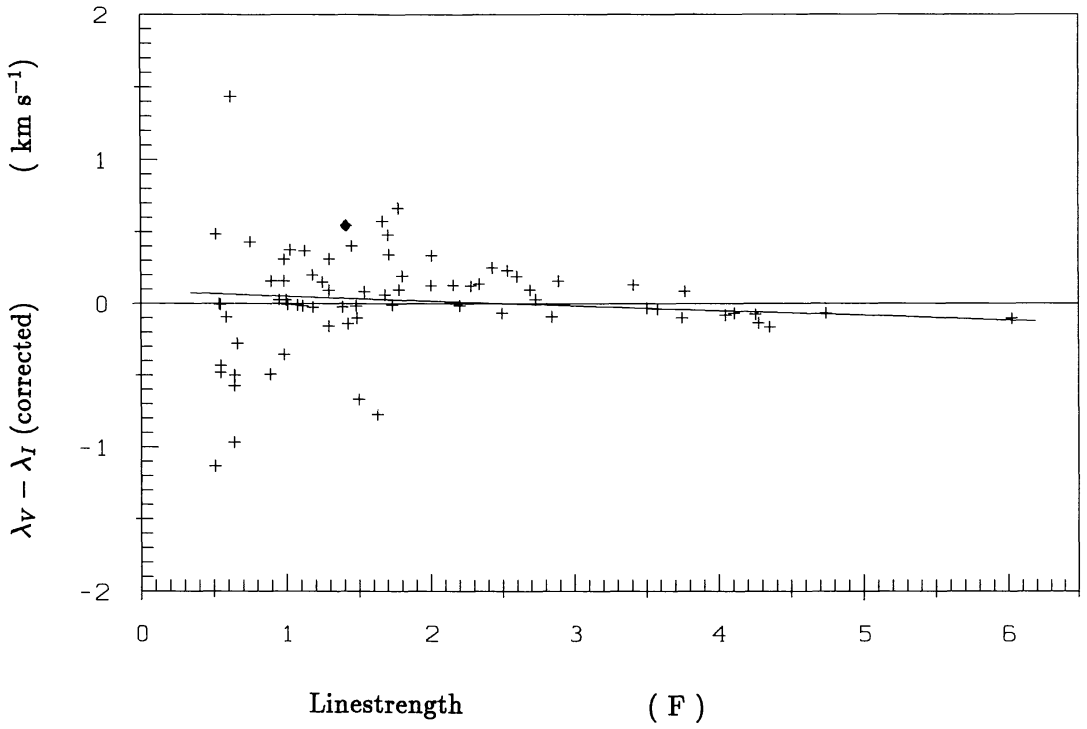

Fig. 5. Difference between the Stokes V zero-crossing wavelength and Stokes I core wavelength, $\lambda_V - \lambda_I$, *vs.* line strength of the I profile, S_I. The blueshift of λ_I due to the solar granulation has been compensated (Nadeau 1988). Therefore the plotted velocities represent vertical flows in the magnetic elements relative to the solar center of gravity. A linear regression through the data points is also plotted.

4.2. Siphon Flows

Stokes V profiles of $\lambda 1.5648$ μm and $\lambda 1.5652$ μm, observed with the Kitt Peak infrared array in the vicinity of a neutral line, as well as the field strengths and velocities derived from them are plotted in Figure 6 (Rüedi *et al.* 1992*b*). Near the neutral line, which intersects the spectrograph slit close to spectrum No. 8, the profiles have an anomalous, highly asymmetric shape. According to Figure 6 the two magnetic components contributing to these anomalous profiles have different field strengths and line-of-sight velocities. The negative polarity has a higher field strength [$B(z = 0) = 1,500$ G] and a *downflow* of $\approx 1\,\mathrm{km\ s^{-1}}$, while the positive polarity has $B(z = 0) = 1,200$ G and an *upflow*. This correlation between field strength and velocity corresponds to exactly the theoretically predicted spectral signature of siphon flows. Although siphon flows along solar magnetic loops have been the subject of extensive theoretical study (*e.g.*, Meyer and Schmidt 1968, Cargill and Priest 1980, 1982, Thomas 1988, Montesinos and Thomas 1989, Thomas and Montesinos 1990, 1991, 1993, Degenhardt 1989, 1991), only 1.5 μm observations have so far provided convincing evidence for their existence in the solar atmosphere.

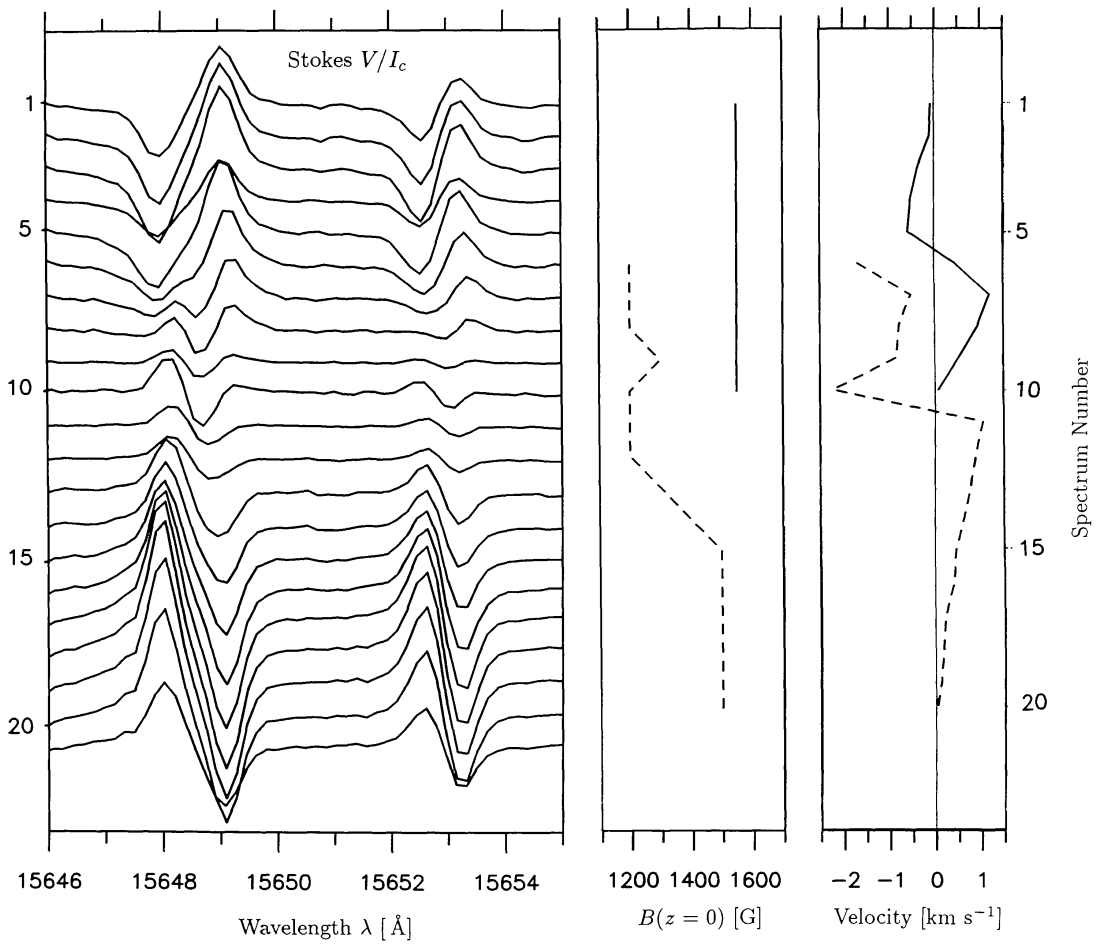

Fig. 6. a) Stokes V spectra at different positions along the slit (each spectrum is offset by 2.5″ with respect to its neighbors). The spectra are numbered at the left of the frame. b) Field strength B along the slit. Dashed curve: positive-polarity fields, solid curve: negative-polarity. c) Line-of-sight flow velocities. Positive velocities are directed downward in the atmosphere.

The infrared is particularly suited to the study of siphon flows, since their detection requires the simultaneous measurement of velocity and magnetic field strengths with great accuracy.

Note that peculiar V profiles, similar to the ones discussed above, have been seen in visible spectra of Ap stars (*e.g.*, Babcock 1951, Mathys 1988) and of neutral lines, generally in sunspot penumbrae (*e.g.*, Kjeldseth Moe 1967, Grigojev and Katz 1972, Golovko 1974, Skumanich and Lites 1991, Sánchez Almeida and Lites 1992). The presence of such peculiar Stokes V profiles has sometimes been referred to as the crossover effect. They have generally been explained by superposing mutually shifted profiles of opposite polarity, although Sánchez Almeida and Lites have been

able to reproduce such profiles using vertical gradients of velocity and magnetic inclination.

5. Summary and Outlook

It is my hope that this review has provided a flavor of the magnetic-field related science possible with near-infrared lines. Even the limited effort spent so far on the interpretation and analysis of near-infrared observations of Zeeman-split lines has returned rich scientific dividends. For example, such investigations have

- enabled accurate, reliable and simple magnetic-field measurements (Livingston 1991, Rabin 1992*a,b*, Solanki *et al.* 1992*a*, *etc.*);
- shown how the field strength is spatially distributed within solar plages (Rabin 1992*a,b*);
- confirmed the prediction that magnetic fields are principally confined by gas pressure (Zayer *et al.* 1989);
- confirmed that approximately 90% of the magnetic flux outside of sunspots is in strong-field form ($\beta(z=0) \leq 1$, Rüedi *et al.* 1992*a*);
- provided the first unequivocal detection of intrinsically weak fields in plages [$\beta(z=0) > 1$, Livingston 1991, Rabin 1992*a,b*, Rüedi *et al.* 1992*a*];
- given estimates of the velocity structure in the deepest layers of magnetic elements: No stationary flows are seen, but a non-stationary RMS velocity of $\approx 1.5\,\mathrm{km\,s^{-1}}$ is detected (Muglach and Solanki 1992);
- set limits on the continuum brightness of magnetic elements (Muglach and Solanki 1992);
- provided the first positive detection of a siphon flow (Rüedi *et al.* 1992*b*);
- measured accurate values of the magnetic field in all parts of sunspots, including the outer edge of the penumbra (McPherson *et al.* 1992, Kopp and Rabin 1992, Solanki *et al.* 1992*b*);
- ruled out return-flux models of sunspots (Solanki *et al.* 1992*b*, Solanki and Schmidt, 1992);
- measured the Evershed flow in the deepest photospheric layers (McPherson *et al.* 1992);
- extended the correlation between temperature and field strength to the whole sunspot (Kopp and Rabin 1992) and provided an estimate of the Wilson depression throughout the sunspot (Solanki *et al.*, in preparation);
- shown that sunspot penumbrae are deep (Solanki *et al.* 1993, Solanki and Schmidt 1992),
- suggested that magnetic elements (Zayer *et al.* 1989) and sunspots (Solanki and Schmidt, 1992) are bounded by current sheets.

Although the above list is already quite long, the near-infrared Zeeman-split lines are only beginning to fulfil their considerable promise. Some of the results that I hope will eventually emerge from this line of research are (in no particular order):

- the detection of a convective collapse;
- an accurate determination of the relationship between the field strength and the temperature in solar magnetic elements;

- identification of the nature of the weak-field magnetic component seen by *e.g.*, Rüedi *et al.* (1992*a*);
- estimates of, or at least limits on, the field strength of intranetwork fields;
- improved limits on (or an outright detection of) a possible turbulent magnetic field (whose presence is suggested by Hanle effect measurements, Stenflo 1982, Faurobert-Scholl 1992);
- a better knowledge of the properties and the frequency of siphon flows;
- accurate (*i.e.*, stray-light independent) field strengths of pores;
- an estimate of the strongest field strengths possible in sunspot photospheres;
- an improved understanding of the nature of the Evershed effect (*e.g.*, is the flow visible in the superpenumbral canopy?);
- many surprises!

References

Avrett E.H., 1993, these proceedings.
Babcock H.W.: 1951, *Astrophys. J.* **114**, 1.
Beckers J.M., Schröter E.H.: 1968, *Solar Phys.* **4**, 142.
Cargill P.J., Priest E.R.: 1980, *Solar Phys.* **65**, 251.
Cargill P.J., Priest E.R.: 1982, *Geophys. Astrophys. Fluid Dyn.* **20**, 227.
Degenhardt D.: 1989, *Astron. Astrophys.* **222**, 297.
Degenhardt D.: 1991, *Astron. Astrophys.* **248**, 637.
Faurobert-Scholl M.: 1992, *Astron. Astrophys.* **258**, 521.
Fleck B.: 1991, *Rev. Modern Astron.* **4**, 90.
Frazier E.N., Stenflo J.O.: 1972, *Solar Phys.* **27**, 330.
Giovanelli R.G.: 1980, *Solar Phys.* **68**, 49.
Giovanelli R.G., Slaughter C.: 1978, *Solar Phys.* **57**, 255.
Golovko A.A.: 1974, *Solar Phys.* **37**, 113.
Grigorjev V.M., Katz J.M.: 1972, *Solar Phys.* **22**, 119.
Harvey J.W: 1977, in *Highlights of Astronomy*, E.A. Müller (ed.), Vol. 4, Part II, p. 223.
Harvey J.W., Hall D.: 1971, in *Solar Magnetic Fields*, R. Howard (ed.), Reidel, Dordrecht, p. 279.
Harvey J.W., Hall D.: 1975, *Bull. Amer. Astron. Soc.* **7**, 459.
Harvey J.W., Livingston W., Slaughter C.: 1972, in *Line Formation in the Presence of Magnetic Fields*, High Altitude Obs., NCAR, Boulder, CO, p. 227.
Hasan S.S.: 1984, *Astrophys. J.* **285**, 851.
Hasan S.S.: 1985, *Astron. Astrophys.* **143**, 39.
Howard R.W., Stenflo J.O.: 1972, *Solar Phys.* **22**, 402.
Kjeldseth Moe O.: 1967, in 'Structure and Development of Active Regions', K.O. Kiepenheuer (ed.), , *IAU Symp.* **35**, 202.
Knölker M., Schüssler M.: 1988, *Astron. Astrophys.* **202**, 275.
Kopp G., Rabin D.: 1992, *Solar Phys.* **141**, 253.
Koutchmy S.: 1991, in *Solar Polarimetry*, L. November (ed.), National Solar Obs., Sunspot, NM, p. 237.
Koutchmy S., Zirker J.B., Darvann T., Koutchmy O., Stauffer F., Mann R., Coulter R., Hegwer S.: 1991, in *Solar Polarimetry*, L. November (ed.), National Solar Observatory, Sunspot, NM, p. 263.
Livingston W.: 1991, in *Solar Polarimetry*, L. November (ed.), National Solar Obs., Sunspot, NM, p. 356.
Mathys, G.: 1988, *Astron. Astrophys.* **189**, 179.
McPherson M.R., Lin H., Kuhn J.R.: 1992, *Solar Phys.* **139**, 255.
Meyer F., Schmidt H.U.: 1968, *Zs. Angew. Math. Mech.* **48**, 218.
Montesinos B., Thomas J.H.: 1989, *Astrophys. J.* **337**, 977.
Muglach K., Solanki S.K.: 1992, *Astron. Astrophys.* **263**, 301.
Nadeau D.: 1988, *Astrophys. J.* **325**, 480.

Osherovich V.A.: 1982, *Solar Phys.* **77**, 63.
Parker E.N.: 1978, *Astrophys. J.* **221**, 368.
Rabin D.: 1992*a*, *Astrophys. J.* **390**, L103.
Rabin D.: 1992*b*, *Astrophys. J.* **391**, 832.
Rabin D.: 1993, these proceedings.
Rabin D., Jaksha D., Plymate C., Wagner J., Iwata K.: 1991, in *Solar Polarimetry*, L. November (ed.), National Solar Observatory, Sunspot, NM, p. 361.
Rüedi I., Solanki S.K., Livingston W., Stenflo J.O.: 1992*a*, *Astron. Astrophys.* **263**, 323.
Rüedi I., Solanki S.K., Rabin D.: 1992*b*, *Astron. Astrophys.* **261**, L21.
Rutten R. and Carlsson, M.: 1993, these proceedings.
Saar S.H.: 1993, these proceedings.
Sánchez Almeida J., Lites B.W.: 1992, *Astrophys. J.* **398**, 359.
Schüssler M.: 1990, in 'Solar Photosphere: Structure, Convection and Magnetic Fields', J.O. Stenflo (ed.), , *IAU Symp.* **138**, 161.
Skumanich, A., Lites, B.W.: 1991, in *Solar Polarimetry*, L. November (ed.), National Solar Observatory, Sunspot, NM, p. 307.
Solanki S.K.: 1986, *Astron. Astrophys.* **168**, 311.
Solanki S.K., Pahlke K.D.: 1988, *Astron. Astrophys.* **201**, 143.
Solanki S.K., Schmidt H.U.: 1992, *Astron. Astrophys.* submitted.
Solanki S.K., Stenflo J.O.: 1986, *Astron. Astrophys.* **170**, 120.
Solanki S.K., Keller C., Stenflo J.O.: 1987, *Astron. Astrophys.* **188**, 183.
Solanki S.K., Rüedi I., Livingston W.: 1992*a*, *Astron. Astrophys.* **263**, 312.
Solanki S.K., Rüedi I., Livingston W.: 1992*b*, *Astron. Astrophys.* **263**, 339.
Solanki S.K., Rüedi I., Livingston W., Schmidt H.U.: 1993, these proceedings.
Spruit H.C.: 1979, *Solar Phys.* **61**, 363.
Spruit H.C., Zweibel E.G.: 1979, *Solar Phys.* **62**, 15.
Spruit H.C., Van Ballegooijen A.A., Title A.M.: 1987, *Solar Phys.* **110**, 115.
Steiner O.: 1993, these proceedings.
Steiner O., Pizzo V.J.: 1989, *Astron. Astrophys.* **211**, 447.
Stenflo J.O.: 1973, *Solar Phys.* **32**, 41.
Stenflo, J.O.: 1982, *Solar Phys.* **80**, 209.
Stenflo J.O., Harvey J.W.: 1985, *Solar Phys.* **95**, 99.
Stenflo J.O., Solanki S.K., Harvey J.W.: 1987*a*, *Astron. Astrophys.* **171**, 305.
Stenflo J.O., Solanki S.K., Harvey J.W.: 1987*b*, *Astron. Astrophys.* **173**, 167.
Sun W.-H., Giampapa M.S., Worden S.P.: 1987, *Astrophys. J.* **312**, 930.
Thomas J.H.: 1988, *Astrophys. J.* **333**, 407.
Thomas J.H.: 1990, in *Physics of Magnetic Flux Ropes*, C.T. Russell, E.R. Priest, L.C. Lee (eds.), Geophysical Monograph 58, American Geophysical Union, Washington, DC, p. 133.
Thomas J.H., Montesinos B.: 1990, *Astrophys. J.* **359**, 550.
Thomas J.H., Montesinos B.: 1991, *Astrophys. J.* **375**, 404.
Thomas J.H., Montesinos B.: 1993, *Astrophys. J.* in press.
Webb A.R., Roberts B.: 1978, *Solar Phys.* **59**, 249.
Wiehr E.: 1985, *Astron. Astrophys.* **149**, 217.
Wiehr E.: 1987, in *Cool Stars, Stellar Systems, and the Sun*, V., J.L. Linsky, R.E. Stencel (eds.), Lecture Notes in Physics Vol. 291, Springer-Verlag, Berlin, p. 54.
Zayer I., Solanki S.K., Stenflo J.O.: 1989, *Astron. Astrophys.* **211**, 463.
Zayer I., Solanki S.K., Stenflo J.O., Keller C.U.: 1990, *Astron. Astrophys.* **239**, 356.